THE EFFECT OF ASPECT RATIO ON THE BIFURCATION PROPERTIES OF A DOUBLE PARALLEL-CONNECTION LORENZ SYSTEM

Zou Chengzhi (邹成智), *Yang Peicai* (杨培才)

Institute of Atmospheric Physics, Academia Sinica, Beijing

and *Zhou Xiuji* (周秀骥)

Institute of Meteorological Science, State Meteorological Administration, Beijing

Received August 11, 1985

ABSTRACT

A double parallel-connection (DPC) Lorenz system is developed by performing spectrum truncation of the Galerkin series expansion of the two-dimensional Rayleigh-Benard convection equation. Analyses of the equilibrium states indicate that a convective roll stems from a flow with a given wavenumber first losing its stability for a particular aspect ratio β after a stable laminar flow gets unstable; when β has the value β_c able to deprive synchronously two flows with different wavenumbers of stability. occurrences of convective rolls with different wavenumbers depend entirely on the initial conditions, in good agreement with the relevant experimental results. The calculations of the unstablized rolls show that, with a smaller β (as compared with β_c), the DPC Lorenz system has the same bifurcation properties as the ordinary Lorenz system; for a moderate β, the system has very complicated periodic, quasi-periodic and phase-locking motions; for a larger β, it results in intermittent chaos and causes mean flows with different numbers of vortices to occur alternately with time. All these indicate that β has substantial effect on the two Lorenz systems coupled through parallel connection in their interaction and the results.

I. INTRODUCTION

In the convective experiments the ratio of a boundary length L to a height H is an aspect ratio denoted as β, which plays an important role in the establishment of thermal convective rolls and turbulence. Davis (1967)[1] made an investigation of the effect of β upon the number of rolls. The results show that, there is a corresponding wavenumber for any β; when the Rayleigh number gets above a threshold R_c, the flow of the wavenumber becomes unstablized first, thus giving rise to the same number of rolls, which is supported through experiments by Stork and Müller (1972)[2]. They found that when β approaches values capable of making two currents of different wavenumbers unstablized simultaneously, the numbers of rolls observed may differ in different times of experiment under the same external conditions. This was also obtained by Platten and Legros (1984)[3], a problem that cannot be worked out by the linearity theory.

Observations of the effect of β on the set-up of turbulence should be briefly reviewed.

Three values of β were tested in the cylinder convective experiments by Ahlers and Behringer (1978)[4]. By altering the Prandtl number and aspect ratio in a Bénard convective experiment, Gollub and Benson (1980)[5] observed a variety of approaches to turbulence which can be generally reduced to three accepted types of mechanisms leading to chaos: i) a mechanism by which chaos takes place through an unlimited number of period-doubling bifurcations (Feigenbaum, 1978, 1979)[6]; ii) a mechanism causing chaos to happen when quasi-periodic motions with independent frequencies become unstable (Ruelle et al., 1971)[7,8]; and iii) a mechanism in which a saddle point bifurcation and intermittent chaos occur (Pomeau and Manneville, 1971)[9].

In this study, by making the spectrum truncation of the Galerkin series expansion a DPC Lorenz system is built up, a system constructed in a coupled parallel connection way consisting of two Lorenz equations describing a single-wave motion. A discussion is made of the influence of β upon the bifurcation properties of the system. Section II treats the establishment of the system together with its general features. In Sections III and IV the properties of the steady state solution and its physical significance are dealt with and compared qualitatively with the experimental results. In the subsequent sections a discussion is made of the bifurcations of the system after the solution becoming unstablized.

II. THE ESTABLISHMENT OF THE DPC LORENZ SYSTEM AND ITS GENERAL PROPERTIES

The dimensionless equations for the two-dimensional Rayleigh-Bénard convective behavior have the forms[3,11]

$$\begin{cases} \dfrac{\partial \nabla^2 \psi}{\partial t} = -\left(\dfrac{\partial \psi}{\partial x} \dfrac{\partial \nabla^2 \psi}{\partial z} - \dfrac{\partial \psi}{\partial z} \dfrac{\partial \nabla^2 \psi}{\partial x} \right) + P \dfrac{\partial \theta}{\partial x} + P \nabla^4 \psi , \\ \dfrac{\partial \theta}{\partial t} = -\left(\dfrac{\partial \psi}{\partial x} \dfrac{\partial \theta}{\partial z} - \dfrac{\partial \psi}{\partial z} \dfrac{\partial \theta}{\partial x} \right) + R \dfrac{\partial \psi}{\partial x} + \nabla^2 \theta, \end{cases} \tag{1}$$

where ψ denotes streamfunction; θ departure of temperature from a linear profile; P and R are the Prandtl and Rayleigh number, respectively. For the equations the boundary conditions can be set to be

$$\begin{cases} \psi = \Delta\psi = \theta = 0, & z = 0, \pi \\ \psi = \Delta\psi = \dfrac{\partial \theta}{\partial x} = 0, & z = 0, \beta\pi \end{cases} \tag{2}$$

in which β is aspect ratio ($a = 1/\beta$ will be used in equations hereafter). Through the expansion of the Galerkin series the solutions of Eqs. (1) and (2) can be put into the forms

$$\psi = \sum_{m=1}^{\infty} \sum_{n=1}^{\infty} \varphi_{mn}(t) \sin(amx) \sin(nz) ,$$

$$\theta = \sum_{m=0}^{\infty} \sum_{n=1}^{\infty} \theta_{mn}(t) \cos(amx) \sin(nz) . \tag{3}$$

Inserting (3) into (1), one can obtain a set of infinite-dimensional ordinary differential equations describing the amplitude evolution of the wave components φ_{mn}(t) and θ_{mn}(t)[11,12], namely,

$$\dot{\varphi}_{mn}=-\frac{a}{4A(m,n)}\Big\{-\sum_{\substack{P+q=m\\ i+j=n}}(-Pj+qi)A(q,j)\varphi_{Pi}\varphi_{qj}+\sum_{\substack{P+q=m\\ |i-j|=n}}\operatorname{sgn}(i-j)(Pj+qi)A(q,j)\varphi_{Pi}\varphi_{qj}-\sum_{\substack{|P-q|=m\\ i+j=n}}\operatorname{sgn}(P-q)(Pj+qi)A(q,j)\cdot\varphi_{Pi}\varphi_{qj}-\sum_{\substack{|P-q|=m\\ |i-j|=n}}\operatorname{sgn}(P-q)(i-j)(Pj-qi)A(q,j)\varphi_{Pi}\varphi_{qj}\Big\}-PA(m,n)\varphi_{mn}+\frac{Pam}{A(m,n)}\theta_{mn},\tag{4}$$

$$\dot{\theta}_{mn}=-\frac{a}{4}\Big\{\sum_{i+j=n}2mj\varphi_{mi}\theta_{oj}+\sum_{|i-j|=n}2\operatorname{sgn}(i-j)mj\varphi_{mi}\theta_{oj}+\sum_{\substack{P+q=m\\ i+j=n}}(Pj-qi)\varphi_{Pi}\theta_{qj}+\sum_{\substack{P+q=m\\ |i-j|=n}}\operatorname{sgn}(i-j)(Pj+qi)\varphi_{Pi}\theta_{qj}+\sum_{\substack{|P-q|=m\\ i+j=n}}(Pj+qi)\varphi_{Pi}\theta_{qj}+\sum_{\substack{|P-q|=m\\ |i-j|=n}}\operatorname{sgn}(i-j)(Pj-qi)\varphi_{Pi}\theta_{qj}\Big\}+Ram\varphi_{mn}-A(m,n)\theta_{mn}$$

$$m=0,1,2,\cdots;\quad n=1,2,3,\cdots,$$

where $A\,(m,\,n)\,=a^2m^2+n^2$, with $a=\,1/\beta$. The solution of the equations above can be obtained only through truncation. In dynamical systems formed by means of different truncations the mechanisms leading to chaos are quite distinctive in quality, which has been demonstrated by comparison of the results of the increasing truncation number by Curry et al.[13] and that of Curry's 14-dimensional[10] with a 33-dimensional model by Zhong et al.[11] These truncations include modes of $m+n$ being even numbers of ψ_{mn} and θ_{mn}. Note that $(m,\,n)$ will be used to denote ψ_{mn} and θ_{mn} hereafter. As indicated by Zhong et al.[11] these modes are, in fact, obtained by truncation of a spectral series excited in succession by the mode (1,1). The idea of the excitation is based on the fact that, if initial disturbance is given to the mode $(m_0,\,n_0)$ only, then all other modes but $\psi_{m_0n_0}$ and $\theta_{m_0n_0}$ are zero. Putting these values into Eq. (4), then some new non-zero modes except $(m_0,\,n_0)$ will come out due to non-linear interaction. If these modes are put into Eq. (4) as initial values, the re-appearance of themselves and other types of modes can be excited as well. Each time when this procedure is done, new modes will be produced, which is referred to as an "excitation". The mode sequence thus excited is as follows:

$$(m_0,n_0)\to(m_0,n_0),(0,2n_0)\to(m_0,n_0),(0,2n_0),(m_0,3n_0)\to$$
$$\to(m_0,n_0),(0,2n_0),(m_0,3n_0),(0,4n_0),(2m_0,4n_0),(2m_0,2n_0),$$
$$(0,6n_0),(m_0,5n_0)\to\cdots$$

If the mode set Λ_k is produced in the Kth excitation, then, from (4)

$$\Lambda_{k+1}=\{(P+q,i+j),\underset{Pj\neq qi}{(P+q,|i-j|)},(|P-q|,i+j),\underset{Pj\neq qi}{(|P-q|,|i-j|)},(i,j)\,|\,(P,q),(i,j)\in\Lambda_k\}.$$

It is easy to prove by an inductive method (see Appendix) that the set totality due to excitation is

$$\sum_{k=0}^{\infty} A_k = A_\infty = \left\{ ((2l+1)m_0, (2k-1)n_0), (2lm_0, 2kn_0), \begin{matrix} k=1,2,\cdots \\ l=0,1,\cdots \end{matrix} \right\},$$

which shows up as a sequence at the cross points in Fig. 1. The Lorenz system is therefore composed of all modes due to the first excitation of (m_0, n_0).

In this paper, by initiating disturbance synchronously at (m_1, n) and (m_2, n) the respective Lorenz systems (m_1, n), $(0, 2n)$ and (m_2, n), $(0, 2n)$ due to the first excitations are developed together with the cross terms $(m_1+m_2, 2n)$ and $(|m_1-m_2|, 2n)$. By neglecting cross terms and retaining (m_1, n) (m_2, n) and $(0, 2n)$, a double Lorenz system is obtained, that is,

$$\begin{aligned} \dot{\varphi}_{m_1n} &= -PA(m_1,n)\varphi_{m_1n} + \frac{Pam_1}{A(m_1,n)}\theta_{m_1n}, \\ \dot{\theta}_{m_1n} &= m_1na\varphi_{m_1n}\theta_{02n} + Ram_1\varphi_{m_1n} - A(m_1,n)\theta_{m_1n}, \\ \dot{\varphi}_{m_2n} &= -PA(m_2,n)\varphi_{m_2n} + \frac{Pam_2}{A(m_2,n)}\theta_{m_2n}, \\ \dot{\theta}_{m_2n} &= m_2na\varphi_{m_2n}\theta_{02n} + Ram_2\varphi_{m_2n} - A(m_2,n)\theta_{m_2n}, \\ \dot{\theta}_{02n} &= -\frac{1}{2}am_1n\varphi_{m_1n}\theta_{m_1n} - \frac{1}{2}am_2n\varphi_{m_2n}\theta_{m_2n} - 4n^2\theta_{02n}. \end{aligned} \tag{5}$$

Note that $m_1=1$, $m_2=2$, $n=1$ and $P=10$ will be used later in this study.

It is apparent from (5) that, if the initial values are $(\varphi^0_{m_1n}, \theta^0_{m_1n}, 0, 0, \theta^0_{02n})$ or $(0, 0, \varphi^0_{m_2n}, \theta^0_{m_2n}, \theta_{02n})$ where $\varphi^0_{m_1n}$ and $\theta^0_{m_1n}$ or $\varphi^0_{m_2n}$ and $\theta^0_{m_2n}$ are not zero concurrently, then Eq. (5) will be degenerated into the systems consisting of φ_{m_1n}, θ_{m_1n}, θ_{02n} or φ_{m_2n}, $\theta_{m_2n}, \theta_{02n}$, which can be termed the subsystem L_1 and L_2, respectively. θ_{02n} is a mode common to L_1 and L_2. Only when the independent modes of L_1 and L_2 have a non-zero initial value will the subsystems interplay, or else they will evolve separately. In this sense, the two subsystems have a coupled parallel connection between themselves and the "on" or "off" of the "switch" depends on whether the initial value is zero or not. (see Fig. 2)

In addition, Eq. (5) has some common properties as the Lorenz system, such as i) symmetry, i. e., $(\varphi_{m_1n}, \theta_{m_1n}) \to (-\varphi_{m_1n}, -\theta_{m_1n})$ and $(\varphi_{m_2n}, \theta_{m_2n}) \to (-\varphi_{m_2n}, -\theta_{m_2n})$; ii) dissipativity, i. e., $\nabla \cdot \mathbf{V} = \frac{\partial \dot{\varphi}_{m_1n}}{\partial \varphi_{m_1n}} + \frac{\partial \dot{\theta}_{m_1n}}{\partial \theta_{m_1n}} + \frac{\partial \dot{\varphi}_{m_2n}}{\partial \varphi_{m_2n}} + \frac{\partial \dot{\theta}_{m_2n}}{\partial \theta_{m_2n}} + \frac{\partial \dot{\theta}_{02n}}{\partial \theta_{02n}} = -(P+1)\times (A(m_1,n)+A(m_2,n)) - 4n^2 < 0$ and iii) boundariness, obtained by making the following Liapunov function:

$$V = R\left(n-\frac{1}{2}\right)A(m_1,n)\varphi^2_{m_1n} + \frac{P}{2}\theta^2_{m_1n} + R\left(n-\frac{1}{2}\right)A(m_2,n)\varphi^2_{m_2n} + \frac{P}{2}\theta^2_{m_2n} + P(\theta_{02n}+2R)^2,$$

then

$$\begin{aligned} \dot{V} &= -2P\Big[R\left(n-\frac{1}{2}\right)A^2(m_1n)\varphi^2_{m_1n} + \frac{1}{2}A(m_1,n)\theta^2_{m_1n} \\ &\quad + R\left(n-\frac{1}{2}\right)A^2(m_2,n)\varphi^2_{m_2}n + \frac{1}{2}A(m_2,n)\theta^2_{m_2n} + 4n^2(\theta_{02n}+R)^2 - 4n^2R^2\Big] \\ &= -2P[f(V) - 4n^2R^2]. \end{aligned}$$

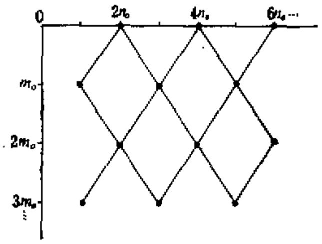

Fig. 1. Schematical illustration of A_∞. $(x, y) \in A_\infty$ if (x, y) is a cross point of two lines.

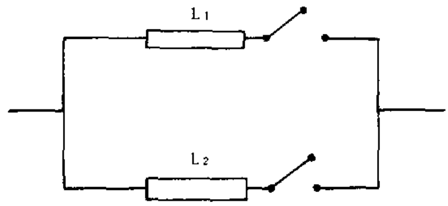

Fig. 2. The DPC Lorenz system is shown schematically. The "circuit" is closed when the initial value is not zero.

If a point is beyond the curved surface $f(v)=4n^2R^2$, then $f(v)>4n^2R^2$, leading to $\dot{V}<0$, thus making the solution bounded[14].

III. THE EQUILIBRIUM STATES AND THEIR STABILITY OF THE DPC LORENZ SYSTEM

By setting the right side of (5) to be zero and solving the corresponding algebraic equations, we have the equilibrium states (ES), which depend strongly on a. Fig. 3 illustrates a curve relating R_c to a, with $a_c=n^2/[m_1^{2/3}m_2^{2/3}(m_1^{2/3}+m_2^{2/3})]=0.49343$, $R_{c_1}=\frac{A^3(m_1,n)}{a^2m_1^2}$, $R_{c_2}=\frac{A^3(m_2,n)}{a^2m_2^2}$, and $R_c=\min(R_{c_1},R_{c_2})$.

According to a, the ES solutions can be grouped into two classes: i) $a\neq a_c$, then $R_{c_1}\neq R_{c_2}$ and Eq. (5) has five ES: $C=(0,0,0,0,0)$, $C_{1\pm}=\left(\pm\frac{1}{A(m_1,n)}\sqrt{8(R-R_{c_1})},\ \pm\frac{A(m_1,n)}{am_1}\sqrt{8(R-R_{c_1})},\ 0,0,-\frac{1}{n}(R-R_{c_1})\right)$, $C_{2\pm}=\left(0,0,\pm\frac{\sqrt{8(R-R_{c_1})}}{A(m_2,n)},\ \pm\frac{A(m_2,n)}{am_2}\sqrt{8(R-R_{c_2})},\ -\frac{1}{n}(R-R_{c_2})\right)$; ii) if $a=a_c$, then $R_c=R_{c_1}=R_{c_2}$ and (5) has $C_0=(0,0,0,0,0)$ and a closed elliptical curve $C_L=\left(\frac{1}{A(m_1,n)}\sqrt{8(R-R_c)}\sin x,\ \frac{A(m_1,n)}{am_1}\times\sqrt{8(R-R_c)}\sin x,\ \frac{1}{A(m_2,n)}\sqrt{8(R-R_c)}\cos x,\ \frac{A(m_2,n)}{am_2}\sqrt{8(R-R_c)}\cos x,\ -\frac{1}{n}\times(R-R_c)\right)$ (where $0\leq x\leq 2\pi$ is a parameter and $x=0,\ \frac{\pi}{2},\ \pi,\ \frac{3}{2}\pi$ correspond to C_{1+}, C_{2+}, C_{1-}, C_{2-}), as its ES.

The stability of the ES solutions above are determined in terms of the eigenvalue of the Jacobian matrix of the function on the right side of (5). Analysis indicates that C_0 has five real eigenvalues that are negative when $R<R_c$ so that C_0 is stable; if $R>R_c$, at least one of the five is positive, C_0 being an unstable saddle node. After C_0 becomes unstable it bifurcates into $C_{1\pm}$ or $C_{2\pm}$ or C_L, depending upon a, i. e.,

i) when $a<a_c$, $R_{c_2}<R_{c_1}$, and with C_0 unstablized, $C_{2\pm}$ branches out of C_0 and has five eigenvalues, two of which are negative real and the others are determined in terms of the equation

$$\lambda^3+((P+1)A(m_i,n)+4n^2)\lambda^2+4n^2A(m_i,n)(P+r_i)\lambda + 8Pn^2A^2(m_i,n)(r_i-1)=0, \qquad (6)$$

where $r_i=R/R_{c_i}$, with $i=2$. When $r_2\leqslant r_{c_2}=P\ (P+3+4n^2/A\ (m_2,n))\ (P-1-4n^2/A(m_2,n))^{-1}$, Eq. (6) gives three roots that have negative real parts, implying the stability of $C_{2\pm}$. When $R>R_{c_1}$, $C_{1\pm}$ also bifurcates from C_0, with one of its eigenvalues being positive real, meaning that $C_{1\pm}$ are never stable, as shown in Fig. 4. A comparison of the results of the Lorenz system[15] with this case indicates that the steady state (SS) nature of (5) can be fully described by L_2.

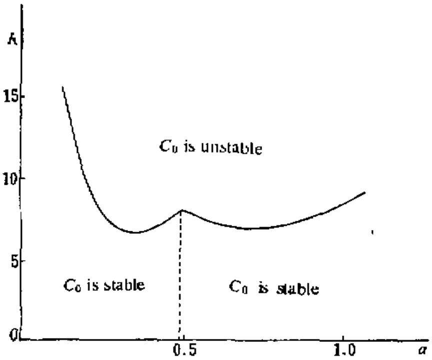

Fig. 3. A curve showing the relation of R_c to a.

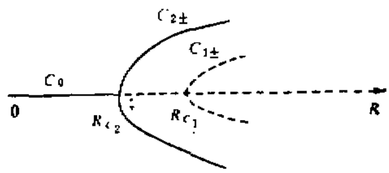

Fig. 4. A diagram of the bifurcation of the ES solutions with $a<a_c$.

ii) when $a>a_c$, $R_{c_1}<R_{c_2}$. In the discussion of $a<a_c$, the properties of $C_{2\pm}$ and $C_{1\pm}$ exchanging with each other will fit this case, which means that the SS nature of (5) can be entirely described by L_1.

iii) when $a=a_c$, $R_c=R_{c_1}=R_{c_2}$. C_L comes out of C_0 after it gets unstable. C_L is a nonisolated equilibrium state, the first critical case of Liapunov[14], always with a zero eigenvalue for each point. The other four eigenvalues are given by Eq. (7):

$$\begin{aligned}&\lambda^4+[(P+1)(A(m_1,n)+A(m_2,n)+4n^2]\lambda^3+\{(P+1)[(P+1)A(m_1,n)A(m_2,n)\\&+4n^2(A(m_1,n)+A(m_2,n)]+4n^2(r-1)[A(m_1,n)\sin^2x+A(m_2,n)\cos^2x]\}\lambda^2\\&+[4n^2(P+1)(P+r)A(m_1,n)A(m_2,n)+8n^2P(r-1)(A^2(m_1,n)\sin^2x\\&+A^2(m_2,n)\cos^2x)]\lambda+8n^2(P+1)P(r-1)A(m_1,n)A(m_2,n)\\&\times[A(m_1,n)\sin^2x+A(m_2,n)\cos^2x]=0\end{aligned} \qquad (7)$$

where $r=R/R_c$. Now we set (7) to have the form $\lambda^4+a_1\lambda^3+a_2\lambda^2+a_3\lambda+a_4=0$, where all coefficients have to satisfy the Routh-Hurwitz conditions for all λ to possess a negative real part[17]. These conditions are:

i) $D_1=a_1\geqslant 0$,

ii) $D_2=\begin{vmatrix} a_1 & a_3 \\ 1 & a_2 \end{vmatrix}=a_1a_2-a_3\geqslant 0$,

iii) $D_3=\begin{vmatrix} a_1 & a_3 & a_5 \\ 1 & a_2 & a_4 \\ 0 & a_1 & a_3 \end{vmatrix}=\begin{vmatrix} a_1 & a_3 & 0 \\ 1 & a_2 & a_4 \\ 0 & a_1 & a_3 \end{vmatrix}=a_1a_2a_3-a_3^2-a_1^2a_4\geqslant 0,$

iv) $D_4=\begin{vmatrix} a_1 & a_3 & a_5 & a_7 \\ 1 & a_2 & a_4 & a_6 \\ 0 & a_1 & a_3 & a_5 \\ 0 & 1 & a_2 & a_4 \end{vmatrix}=a_4D_3\geqslant 0.$

If any of these is not satisfied, then positive real parts will occur in the roots. For Eq. (7), Cond. i) is satisfied and, when $r>1$ and Cond. iii) is satisfied, the same is true of iv). In terms of $D_2=0$ and $D_3=0$, the critical Rayleigh number $r_{c_2}(x)$ and $r_{c_3}(x)$ can be obtained respectively. Comparison shows that $r_{c_3}(x)<R_{c_2}(x)$, with $0\leqslant x\leqslant 2\pi$. Let $r_c(x)=\min\ (r_{c_2}(x),\ r_{c_3}(x))=r_{c_3}(x)$ and for $R_c<R<R_c\ r_c(x)$, Conds. ii) and iii) are satisfied, leading to the fact that all roots of (7) have a negative real part. A curve of the relation of $r_c(x)$ to x is shown in Fig. 5, where one can see that, when $r<r_c(0)=$

$P\left(P+3+\dfrac{4}{A(2,1)}\right)\left(P-1-\dfrac{4}{A(2,1)}\right)^{-1}=21.548$, the eigenvalue of each point of C_L has a negative real part (excluding the zero one), which indicates that C_L is stable according to the Liapunov theorem of the first critical case[14]. However, C_L is one-dimensionally undeterminable, meaning that any initial value given in the neighborhood of C_L will move to and stay at some point of C_L, with the initial value specifying the movement to the full extent.

IV. THE PHYSICAL SIGNIFICANCE OF THE STEADY STATE SOLUTIONS OF (5)

The significance of the SS solutions of (5) can be interpreted by means of the so-called method of small-parameter expansion. As shown in linearity theory, for a certain a there is $R_c=\inf\limits_{m,n} A^3(m,n)/a^2m^2=\dfrac{A^3(m_0,n_0)}{a^2m_0^2}$. When $R<R_c$, Eqs. (1) and (2) have only one steady solution of a stationary laminar flow $\psi=\theta=0$. And when $R>R_c$, the wave with the wavenumber (m_0, n_0) loses its stability first of all, whose solutions can be found in terms of small-parameter method[15], if the difference of $R-R_c$ is small.

Let

$$R=R_0+\varepsilon R_1+\varepsilon^2R_2+\cdots=\sum_{i=0}^{\infty}\varepsilon^iR_i,$$

$$\psi=\varepsilon\psi^{(0)}+\varepsilon^2\psi^{(1)}+\varepsilon^3\psi^{(2)}+\cdots=\sum_{i=1}^{\infty}\varepsilon^i\psi^{(i-1)}, \tag{8}$$

$$\theta=\varepsilon\theta^{(0)}+\varepsilon^2\theta^{(1)}+\varepsilon^3\psi^{(2)}+\cdots=\sum_{i=1}^{\infty}\varepsilon^i\theta^{(i-1)},$$

where $R_0=R_c$, ε is a small parameter. Putting (8) into (1), we have

$$\begin{cases} \dfrac{\partial \nabla^2 \psi^{(K)}}{\partial t} = \displaystyle\sum_{i+j=K-1} \left(\frac{\partial \psi^{(i)}}{\partial z} \frac{\partial \nabla^2 \psi^{(j)}}{\partial x} - \frac{\partial \psi^{(i)}}{\partial x} \frac{\partial \nabla^2 \psi^{(j)}}{\partial z} \right) + P \frac{\partial \theta^{(K)}}{\partial x} + P \nabla^4 \psi^{(K)}, \\ \dfrac{\partial \theta^{(K)}}{\partial t} = \displaystyle\sum_{i+j=K-1} \left(\frac{\partial \psi^{(i)}}{\partial z} \frac{\partial \theta^{(j)}}{\partial x} - \frac{\partial \psi^{(j)}}{\partial x} \frac{\partial \theta^{(i)}}{\partial z} \right) + R_0 \frac{\partial \psi^{(K)}}{\partial x} + \sum_{\substack{i+j=K \\ j<K}} R_i \frac{\partial \psi^{(j)}}{\partial x} + \nabla^2 \theta^{(K)}, \end{cases} \tag{9}$$

$$K = 1, 2, 3, \cdots$$

and

$$\begin{cases} \dfrac{\partial \nabla^2 \psi^{(0)}}{\partial t} = P \dfrac{\partial \theta^{(0)}}{\partial x} + P \nabla^4 \psi^{(0)}, \\ \dfrac{\partial \theta^{(0)}}{\partial t} = R_0 \dfrac{\partial \theta^{(0)}}{\partial x} + \nabla^2 \theta^{(0)}. \end{cases} \tag{10}$$

The latter is a system of linear equations, whose solutions can be set to have the form of Eq. (3) according to the boundary conditions. Inserting the form into (10), we obtain a set of equations whose ES solutions satisfy:

$$\begin{cases} -PA(m,n)\varphi^{(0)}_{mn} + \dfrac{Pam}{A(m,n)} \theta^{(0)}_{mn} = 0, \\ R_0 am \varphi^{(0)}_{mn} - A(m,n)\theta^{(0)}_{mn} = 0. \\ (n = 1, 2, \cdots;\ m = 0, 1, 2, \cdots.) \end{cases} \tag{11}$$

We can know from (11) that all but modes $\varphi^{(0)}_{m_0 n_0}$ and $\theta^{(0)}_{m_0 n_0}$ are zero. Hence with the zero-order approximation $\psi^{(0)} = \varphi^{(0)}_{m_0 n_0} \sin(am_0 x) \sin(n_0 z)$ and $\theta^{(0)} = \theta^{(0)}_{m_0 n_0} \cos(am_0 x) \sin(n_0 z)$ as a starting point, Eq. (9) is put into use repeatedly as K increases, leading to the fact that (9) are linear equations for $\psi^{(K)}$ and $\theta^{(K)}$ with the solutions in the form of (3). It is apparent from (9) that, owing to the non-linear interplay of the SS solutions of lower-order, some new non-zero modes in the SS solutions of any order of $\psi^{(K)}$ and $\theta^{(K)}$ will come about and these modes are the same as those yielded in the *K*th excitation as described in Section II, that is,

$$\varphi^{(0)}_{m_0 n_0},\ \theta^{(0)}_{m_0 n_0} \to \varphi^{(1)}_{m_0 n_0},\ \theta^{(1)}_{m_0 n_0},\ \theta^{(1)}_{02 n_0} \to \varphi^{(2)}_{m_0 n_0},\ \theta^{(2)}_{m_0 n_0}, \theta^{(2)}_{02 n_0},\ \varphi^{(2)}_{m_0 3 n_0},\ \theta^{(2)}_{m_0 3 n_0}\ .$$

It follows that when R approaches R_c, the Lorenz system corresponds to the first-approximation description of the convective equation. Kuo has got a 9th-order approximation[18], the result being in good agreement with experimentation.

As a changes, (m_0, n_0) alters accordingly. Eq. (5) includes two independent Lorenz first-approximation modes (m_1, n), $(0, 2n)$ and (m_2, n), $(0, 2n)$. Therefore, the stable C_0 is able to describe the stationary laminar flow when $a \neq a_c$, while the steady $C_{1\pm}$ and $C_{2\pm}$ have ability to describe convective rolls produced mainly by the flows with wavenumbers (m_1, n) and (m_2, n) respectively, as illustrated in Fig. 6. When $a = a_c$, $R_c = \inf\limits_{m,\,n} \dfrac{A^3(m,n)}{a^2 m^2} = \dfrac{A^3(m_1,n)}{a^2 m_1^2} = \dfrac{A^3(m_2,n)}{a^2 m_2^2}$, and hence $\psi^{(0)}$ and $\theta^{(0)}$ include modes (m_1, n) and (m_2, n) while the first-approximation SS solutions $\psi^{(1)}$ and $\theta^{(1)}$ include modes (m_1, n), (m_2, n), $(0, 2n)$, $(|m_1 - m_2|, 2n)$, $(m_1 + m_2, 2n)$. Therefore the modes truncated in this article are not really a first-approximation for $a = a_c$. However, the results can be used to qualitatively interpret the phenomena observed in the experimentation indicated in Refs. [2] and [3] to a great extent. For $a=a_c$, the SS solution is a stable closed elliptical curve containing $C_{1\pm}$ and $C_{2\pm}$. The number of rolls formed can be either (m_1, n) or (m_2, n). All the two patterns shown in Fig. 6 will take place, but which state will emerge depends completely on initial values. Thus, if a is equal to such critical values, then two different numbers of rolls may occur in two different times of experiment, despite the external conditions being the same.

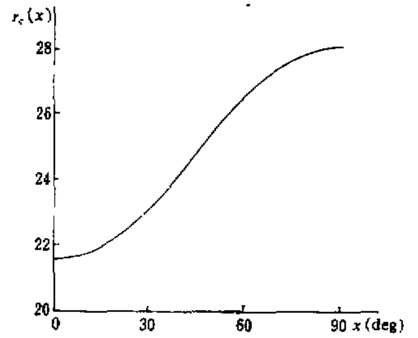

Fig. 5. The curve of the relation of r_c (x) to x.

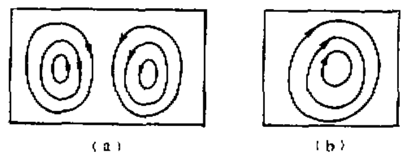

Fig. 6. Convective rolls yielded chiefly by the flows with wavenumber (2,1) (left) and (1,1) (right).

V. THE BIFURCATION PROPERTIES OF NON-STEADY-STATE SOLUTIONS OF EQ. (5) FOR $a=a_c$

The stability of the ES of (5) and the physical significance have been investigated in previous sections. Now we turn to the features of the solution around a point where a steady state gets unstablized, which needs a computer to solve (5). For $a=a_c$, it is obvious from Fig. (5) that when $r>r_c(90°)=P\left(P+3+\frac{4n^2}{A(m_1,n)}\right)\left(P-1-\frac{4n^2}{A(m_2,n)}\right)^{-1}\approx 28.04$, C_L becomes fully unstablized, meaning that at least one of the eigenvalues of each point at C_L has a positive real part. Then, if an initial value, say (0,1,0,1,0) is given, the solution of (5) will be found to move finally to a limit cycle τ_0. Fig. 7 depicts frequency spectra of φ_{11} and φ_{21} of τ_0 with $r=29.96$. It can be seen that the basic frequency of τ_0 is f_0, with the subharmonic frequency of L_1 and L_2 being $2f_0$, $4f_0$, $\cdots$ $2Kf_0$ and f_0, $3f_0$, $\cdots$, $(2K-1)f_0$, respectively both with $K=1,2,\cdots$. It follows that τ_0 is symmetrical: $L_1(t)=L_1\left(t+\frac{T_0}{2}\right)$ and $L_2(t)=-L_2\left(t+\frac{T_0}{2}\right)$ with the period of $T_0=1/f_0$.

Tracking τ_0 in the direction of r increases reveals that its symmetry is damaged when $r\geqslant r_1\approx 33.3$. Fig. 8 illustrates the frequency spectrum of φ_{11} for $r=33.35$. Its comparison with Fig. 7 shows that, because of the damage of the symmetry, the subharmonic frequencies of L_1 and L_2 will contain a whole multiple of f_0, i. e., nf_0, with $n=1,2,3,\cdots$. When $r\geqslant r_2\approx 33.42$, τ_0 becomes unstable and comes into chaos (see Fig. 8). After the periodic solution has disappeared, however, no intermittent chaos or bifurcation happens. Therefore, it is necessary to explain how τ_0 gets unstablized.

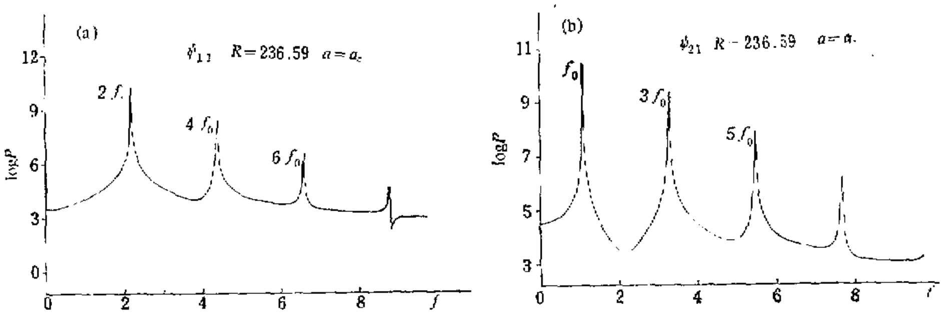

Fig. 7. Periodic solutions for $a=a_c$ and $r=29.96$. (a) and (b) show the *frequency spectra of* φ_{11} *and* φ_{21}, *respectively.*

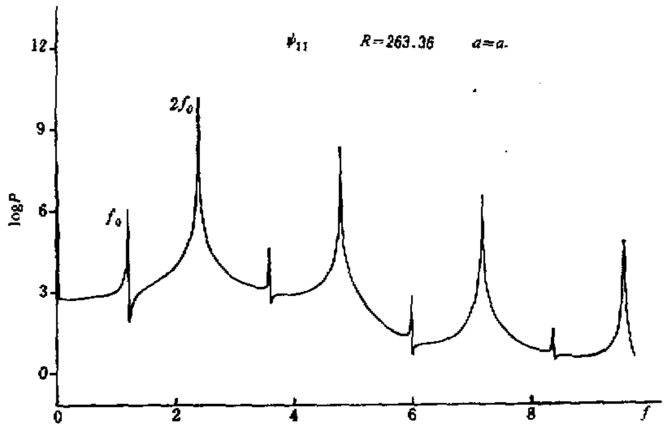

Fig. 8. The frequency spectrum of φ_{11} for $a=a_c$ and $r=33.35$.

In fact, there is a chaos solution concurrently with τ_0, whose attractive domain is enlarged as r increases. When r is relatively far from r_c (90°), the solution with initial value around the origin will go into a chaos state. Fig. 9 shows the projection of Poincare cross-section[1)] of chaos and the τ_0 onto L_1 for $r=32.8$ and 33.35. As illustrated in this figure, as r increases, τ_0 gets closer and closer to chaos and at $r=r_1$, the intense disturbance of chaos results in "damage of symmetry" of the periodic solution, which, in the end, "collides" with chaos to the full extent and is "swallowed" by the latter at $r=r_2$. At this time the limit-cycle becomes a strange attractor without going through any bifurcation, which is similar to the breaking of tori investigated by Franceschini and Tebaldi[19]. In their case,

1) The Poincare cross-section is defined as $\theta_{12}=-(R-R_c)$.

a stable torus collides with an unstable limit-cycle, the former goes through a "catastrophe", changing to chaos suddenly. Here τ_0 meets with chaos and is swallowed, which is also a "catastrophe".

Now we shall track τ_0 in the direction r decreases. It is found that for $r \leqslant r_{Q_1} \approx 25.3$, τ_0 branches into a two-dimensional quasi-periodic torus τ_1, with basic frequencies f_0 and f_1. Fig. 11a—b illustrates the phase trajectory and frequency spectrum of τ_1 for $r=25.274$, respectively. When $r \leqslant r_{Q_2}=25.18$, τ_1 bifurcates into a three-dimensional quasi-periodic torus τ_2 with basic frequencies f_0, f_1 and f_2. Fig. 11c—d depicts frequency spectrum of τ_2 and the Poincare section. Fig. 10 indicates the variations of f_1 and f_2 with r, but the case of $f_0 \approx 0.94$, being quite constant over the range of the parameters given, is not shown. As seen from the figure, f_1 changes slowly, whereas f_2 varies very fast, and consequently f_0, f_1 and f_2 are three incommensurable frequencies. As shown in Fig. 10, over the interval of $r \in [r_{L_2}, r_{L_1}]$, for $r_{L_2} \approx 25.13$ and $r_{L_1} \approx 25.15$, f_1 is locked at $f_0/8$, that is, a locking phase takes place. Hence there are only two independent frequencies f_1 and f_2 and a three-dimensional torus is fixed at a two-dimensional torus τ_L, which is given in Fig. 11e. When r continues to decrease, a three-dimensional torus is obtained once more, but f_2 will go up instead of going down. When $r \leqslant r_P \approx 25.093$, f_1 is locked at $f_0/9$ and f_2 at f_1, i. e., $f_2=f_1=f_0/9$. In this case a periodic locking phase occurs. Fig. 11f is the Poincare section of τ_P with 18 points on it with $f_1=0.012$ for $r=25.09$. When $r \leqslant r_s \approx 25.086$, τ_P comes into weak chaos, during which time the Poincare section can no longer show a closed cycle, although the motions with f_0 and f_1 still dominate. Fig. 11g indicates the section for $r=25.0857$.

If r keeps diminishing, the periodic locking phase and chaos emerge alternately, which seems analogous to the locking phase of a system of seven-mode equations investigated by Franceschini[20]. Yet it will take more calculations to determine these cases and no further discussion will be held in this study. When $r \leqslant r_d \approx 24.92$, the chaos disappears. In this case solutions of (5) with initial values given stochastically will come to the steady interval of C_L in the long run.

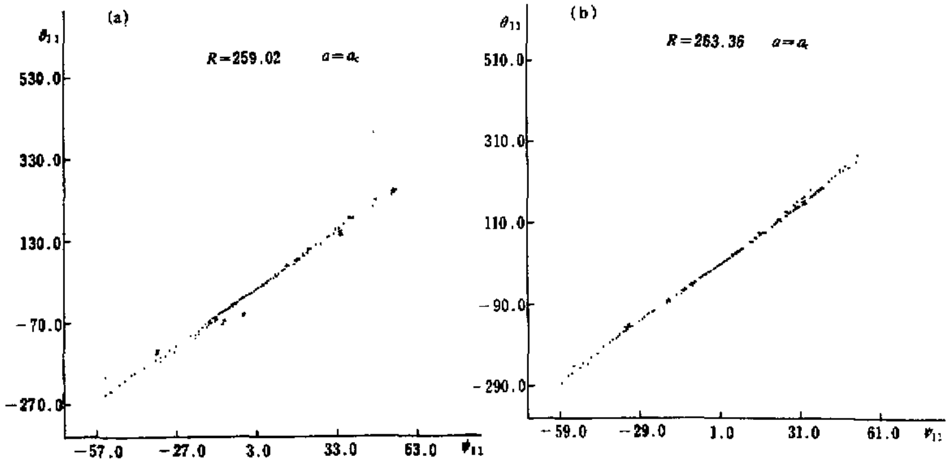

Fig. 9. Poincare section for $r=32.8$ (a) and for $r=33.35$ (b). Cross denotes periodic solutions.

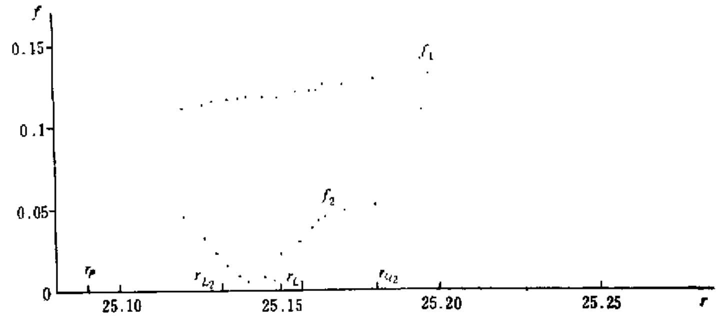

Fig. 10. Curves showing the relation of f_1 and f_2 to r.

It should be noted that f_1 and f_2 in Fig. 10 are determined by performing spectrum analysis of the points on the Poincare section. This is because an extremely large N is required to specify such a frequency as low as f_2 if the sampling points $x(k\Delta)$ with $k=1,2,\cdots$, N of the solution $x(t)$ of (5) are directly used to make spectral analysis. However, if the point sequence $x'(k\Delta')$, $k=1,2,\cdots$, N' on the Poincare section is used for spectral analysis, then a relatively small N' will include a longer-term set of samples and since the effect of f_0 has been reduced, the low frequency like f_2 can be defined more accurately. Δ' is the time difference between two successive points on the Poincare section and varies slightly with time. If the mean Δ' is used as the sampling interval for the analysis, then the frequency obtained will have higher precision. For example, the frequency spectrum of $\varphi_{21}(k\Delta')$ on the Poincare section for $r=25.164$ is shown in Fig. 11h, where $f_1=0.1246$ and $f_2=0.044$ are determined, and from Fig. 11c $f_1=0.1221$ and $f_2=0.0488$ can be obtained, indicating that the relative error of f_1 and f_2 are 2% and 10%, respectively. This is due to the low frequency determined inaccurately from Fig. 11c. Franceschini employed the method to treat the period-doubling of a high-dimensional torus[20].

From the above it can be seen that, when $a=a_c$, Eq. (5) shows a complicated coexistence of many attractors. Fig. 12 displays the variations of attractors versus r schematically. For the sake of intuition the intervals are not given in proportion, with the curve of critical C_L straightened.

VI. THE BIFURCATION PROPERTIES OF NONSTEADY-STATE SOLUTIONS OF EQ. (5) FOR $a \neq a_c$

The properties of the solutions with different a are calculated for $a\neq a_c$ when the steady states become unstable and described as follows.

i) if $a=0.436168 < a_c$, corresponding to $\beta > \beta_c$, then $R_{c_1} > R_{c_2}$ and $C_{1\pm}$ will never be stable as indicated in Section III. For $r_2 > r_{c_2} \approx 22.697$, $C_{2\pm}$ becomes unstablized, when the solutions with initial values given randomly exhibit intermittent chaos. Fig. 13a depicts a one-dimensional return map on the Poincare section that clearly shows the properties of intermittent chaos of the solutions[9]. Fig. 13b—c represents the variations of φ_{11} and φ_{21} with time, showing the oscillation alternately around C_{1-}, C_{2+} and C_{2-}, i. e., the motion of L_1 or L_2 is dominant alternatively[2]. When this happens, there occur mean flows alternately with one and two vortices dominant as time goes on. In this sense, the mean structure of the turbulent state is unsteady and, relatively speaking, L_2 is

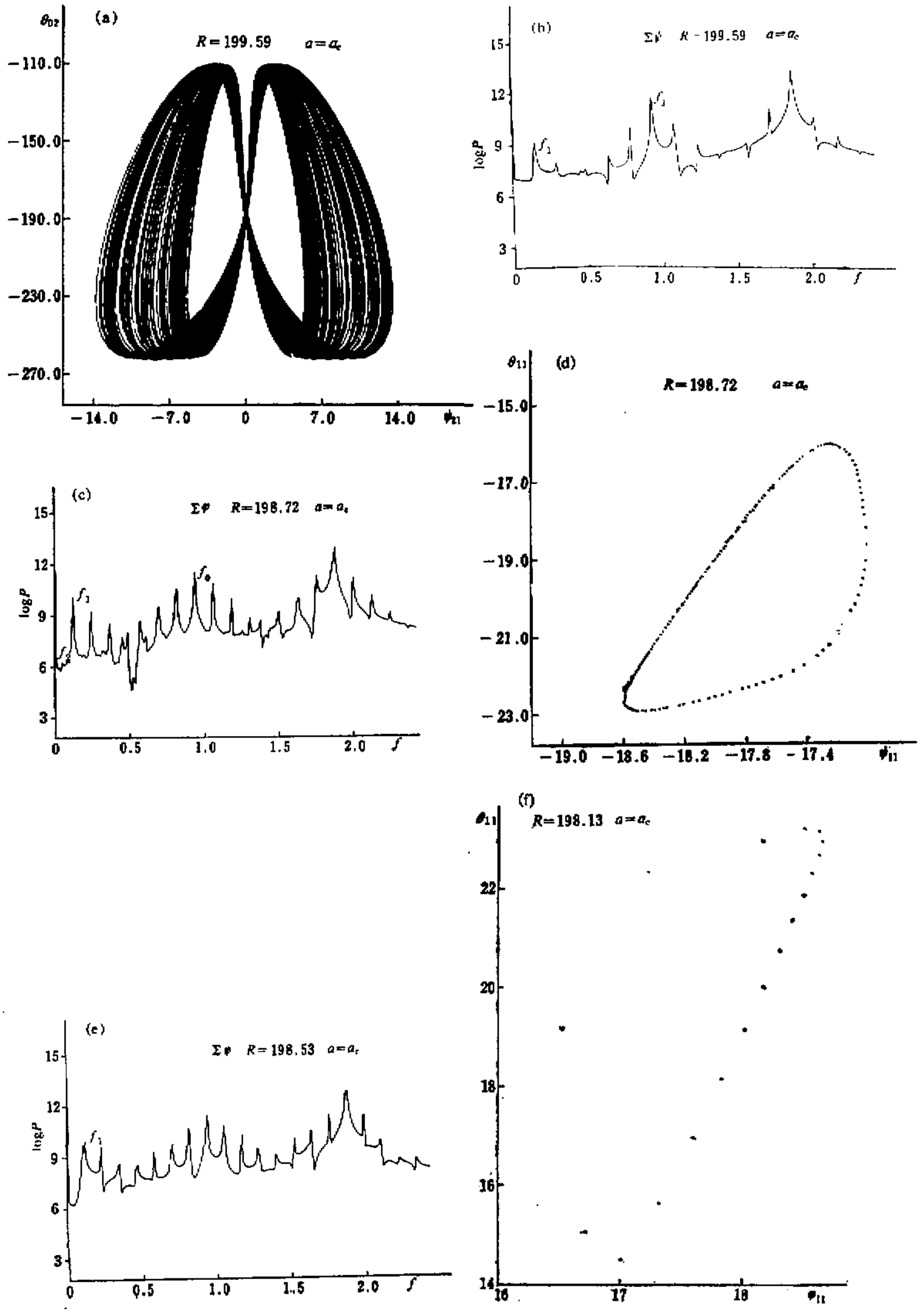
(a)
R=199.59 a=a_c
θ02
−110.0
−150.0
−190.0
−230.0
−270.0
−14.0
−7.0
0
7.0
14.0
ψ11
(b)
Σψ R=199.59 a=a_c
logP
15
12
9
6
3
0
0.5
1.0
1.5
2.0
f
f1
(c)
Σψ R=198.72 a=a_c
logP
f1
(d)
R=198.72 a=a_c
θ11
−15.0
−17.0
−19.0
−21.0
−23.0
−19.0
−18.6
−18.2
−17.8
−17.4
ψ11
(e)
Σψ R=198.53 a=a_c
logP
f1
(f)
R=198.13 a=a_c
θ11
22
20
18
16
14
16
17
18
ψ11

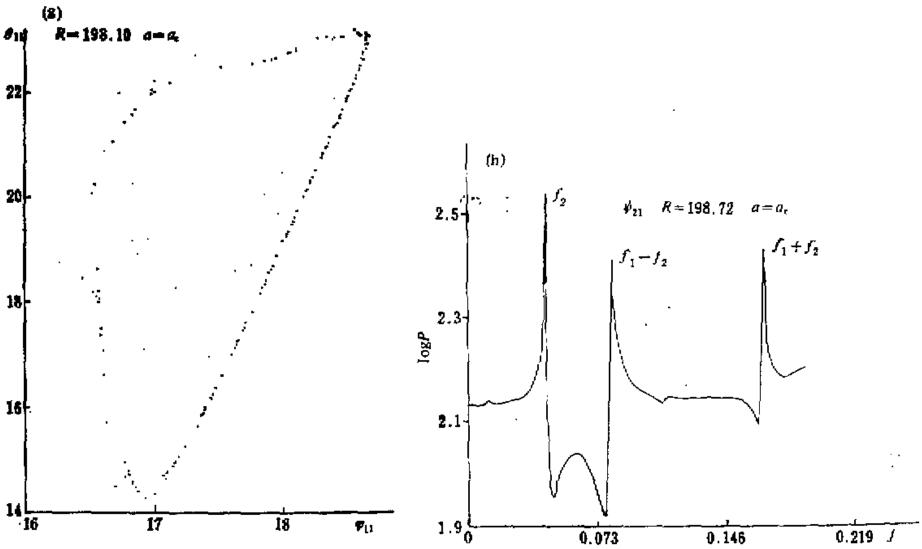

Fig. 11. (a) and (b) show the phase trajectory and frequency spectrum for $r=25.274$, respectively; (c) and (d) the frequency spectrum and Poincare section for $r=25.164$, separately; (e) is the frequency spectrum for $r=25.14$; (f) the Poincare section for $r=25.09$; (g) the Poincare section for $r=25.0857$; (h) the frequency spectrum on the Poincare section for $r=25.164$.

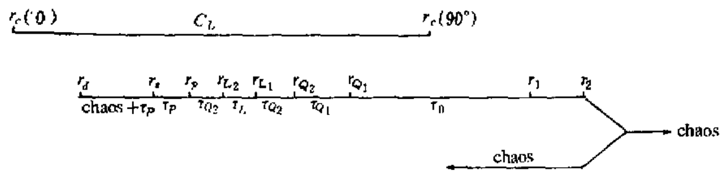

Fig. 12. A diagram showing the variation of attractors versus r, with the straightened C_L being $r_c^{-1}(x)$, i. e., $x=x(r_c)$. For $r>r'$ the points at C_L corresponding to $x>x(r')$ are stable. The parameters used are: $r_c(0)\approx21.55$, $r_c(90°)\approx28.04$, $r_d\approx24.92$, $r_s\approx25.086$, $r_p\approx25.092$, $r_{L_2}\approx25.13$, $r_{L_1}\approx25.15$, $r_{Q_2}\approx25.18$, $r_{Q_1}\approx25.30$, $r_1\approx33.3$ and $r_2\approx$ 33.42.

more active since $C_{2\pm}$ all can occur. This is different from the SS cases for $a=a_e$, as indicated in Sections III and IV, where the number of rolls depends on initial values and remains steady after their formation. And here the case of $a\approx0.44$ illustrates that different numbers of vortex structures show up alternately with time, regardless of any initial value.

2) It can be seen from symmetry that some other initial values may cause oscillations near C_{1+}, C_{2+} and C_{2-}.

As r grows, the mean time that the solution stays around each state is steadily reduced with chaos being strengthened. A three-dimensional (for $r_2 \geqslant 32.9$) and a two-dimensional (for $r_2 \geqslant 33.1$) torus takes place and, when $r \geqslant 34$, periodic solutions occur. It follows that, in the vicinity of $r_2 = 34$, as r_2 decreases the solution goes through a Ruelle-Takens bifurcation scenario, i. e., period→quasi-period→ (locking phase)→chaos.

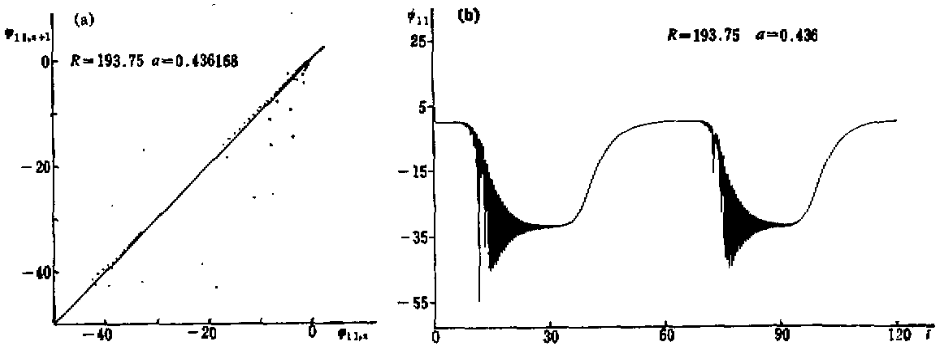

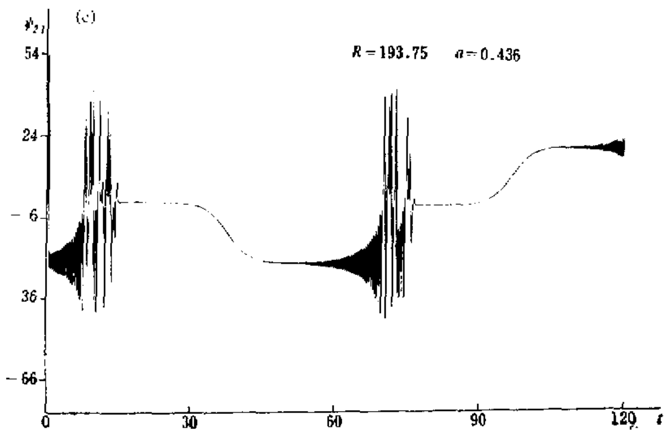

Fig. 13. (a) a one-dimensional return map on the Poincare section: (b) φ_{11} (t); (c) φ_{21} (t), for $a=0.436168$ and $r_2=27$.

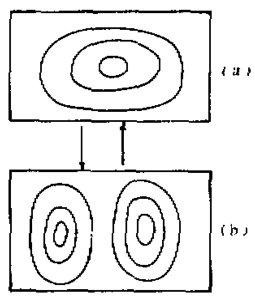

Fig. 14. The mean flows with one and two vortices occur alternately.

Besides, the properties of the solution for $a=1/\sqrt{8}$ are calculated and the result acquired is analogous to the above.

ii) For $a>a_c$, calculation is performed of two points, one at $a=0.52$, closer to a_c and the other at $a=1/\sqrt{2}\approx 0.7071$ farther from a_c. In the former case the point where $C_{1\pm}$ loses its stability is at $r_{c_1}=27.598$, and after $C_{1\pm}$ being unstablized an initial value selected stochastically will give a periodic solution, and further result reveals the similarity of its bifurcation structure to that for $a=a_c$, also with a coexistence of many attractors. If the C_L curve is substituted for $C_{1\pm}$ in Fig. 12, then the bifurcation for $a=0.52$ can be described, only with the values of the parameters slightly changed.

$a=1/\sqrt{2}$ is a widely-used value[10,15], for which β is relatively small. According to the description in Section III, $C_{2\pm}$ is never steady and $r_{c_1}\approx 24.74$ is the point at which $C_{1\pm}$ gets unstable. For $r_1>r_{c_1}$, randomly-chosen initial values bring about chaos. Fig. 15 shows the variations of L_1 and L_2 versus time for $r_1=27$. It is apparent that, as far as the movement of the system is concerned, that of L_1 dominate while L_2 has only tiny amplitude movement in the vicinity of zero, which is quite different from that for a greater β. As indicated in Fig. 14b, a smaller β restricts the development of the mean flow with two vortices and forces it to form a flow having one vortex only (see Fig. 14a). Hence for a smaller β, the mean structure of the turbulent state is steady, i. e., the subsystem L_1 is dominant. Yet, as r increases, L_2 plays a greater and greater role in the motion. When $r=100$, for instance, it is hard to distinguish which of the Lorenz subsystems predominates in the chaos motion.

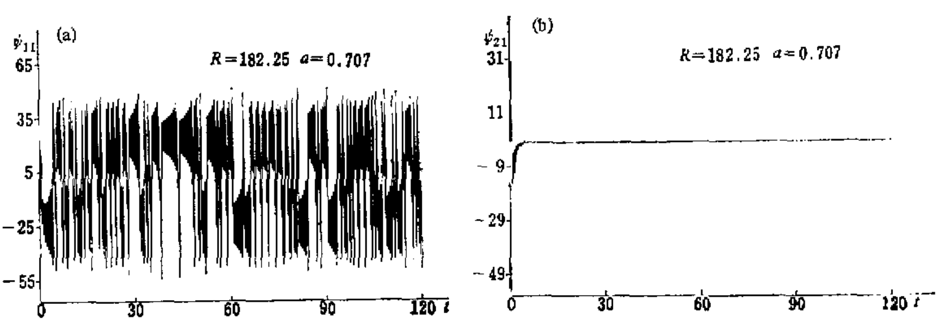

Fig. 15. (a) the diagram of φ_{11} (t); (b) the diagram of φ_{21} (t), for $a=1/\sqrt{2}$ and $r_1=27$.

VII. CONCLUSIONS

By making proper spectrum truncation of the Galerkin series expansion of the two-dimensional Benard convective equation, a simpler DPC Lorenz system is obtained, and thereby the role of the aspect ratio β is discussed in the development of convection. The results are:

(1) the steady state of the DPC system in the neighborhood of the first critical point can be used to describe quite well how the convective rolls result. In particular for $a=a_c$, the system shows a closed cycle of solutions consisting of an unlimited number of steady states, indicating that after a stationary laminar the flow gets unstable, and the formation of rolls with two different wavenumbers will depend entirely on initial conditions. Hence this can lend itself to the qualitative explanation of the experimental results as indicated in Refs. [2] and [3].

(2) As shown in the calculation of the bifurcation properties of nonsteady state solutions, β is a key factor in determining the degree of the interaction between L_1 and L_2. For $\beta=\beta_c$, there coexist several attractors that may merge one into another. In addition, a single attractor has a complex bifurcation structure, i. e. it may be marked by the Ruelle-Takens line: periodic motion→quasi-periodic motion→locking phase →chaos. When β is

greater, intermittent chaos will occur after the steady state gets unstable, and the motions with L_1 and L_2 in the main will happen alternately; when β is smaller and r_1 is not far from r_{c_1}, L_2 plays no role to a great extent and the motion of L_1 predominates, with the bifurcation properties similar to those of the Lorenz system.

Finally, it should be pointed out that the DPC Lorenz system for $a=a_c$ has the same form as the complex Lorenz equation derived from a two-level baroclinic unstable equation or from a self-induced transparency equation in optics when all parameters are real[21]. This shows that such an equation can be induced from a variety of physical phenomena. Of course, it will take still more analyses and calculations to completely reveal the interesting facts and contents of physics involved in such equations.

The authors are grateful to Prof. Hao Bolin and Prof. Qin Yuanxun for their valueable suggestions and comments and also to Mr. Zhong Wenyi for his help in calculations.

APPENDIX

Prove the following by an inductive method:

$$\sum_{i=0}^{\infty} \Lambda_i = \{((2l+1)m_0, (2k-1)n_0), (2lm_0, 2kn_0), l=0,1,\cdots;\ k=1,2,\cdots\}.$$

Proof: Let the set be $\Lambda'_{K,L}$, consisting of the following sequences:

$$(2l_{m_0}, 2k_{n_0}),\ k=1,2,\cdots,K,\ K\geqslant 2;\ l=0,1,\cdots,L, L\geqslant 2;$$

$$((2l+1)m_0, (2k-1)n_0), k=1,2,\cdots K, K\geqslant 2;\ l=0,1,\cdots L, L\geqslant 1.$$

The other terms $(0, 2n_0)$, $(2m_0, 2n_0)$ and (m_0, n_0) are easy to obtain from the first few excitations of (m_0, n_0). Now all we have to do is to prove that $\Lambda'_{K+1,L+1}$ can be deduced from $\Lambda'_{K,L}$. In fact, we may use the sequence $(2m_0, 2kn_0)$, $k=1,2,\cdots,K$, and $(2Lm_0, 2n_0)$; sequence $(2lm_0, 2n_0)$, $l=0,1,\cdots,L$, and $(2m_0, 2kn_0)$; sequence $(2m_0, 2kn_0)$, $k=1,2,\cdots,K$, and $((2L+1)m_0, 2n_0)$; sequence $((2l+1)m_0, n_0)$, $l=0,1,\cdots,L$, and $(2m_0, 2kn_0)$ to get such sequences as $(2(L+1)m_0, 2kn_0)$, $k=2,3,\cdots,K+1$; $(2lm_0, 2(k+1)n_0)$, $l=1,2,\cdots,L+1$; $((2L+3)m_0, (2k-1)n_0)$, $k=2,3,\cdots,K+1$; $((2l+1)m_0, 2(k+1)n_0)$, $l=1,2,\cdots,L+1$, with the aid of the nonlinear term $\sum\limits_{\substack{p+q=m\\ i+j=n}} (Pj-qi)\varphi_{pi}\varphi_{qj}$. The other four modes $(2(L+1)m_0, 2n_0)$, $(0, 2(k+1)n_0)$, $((2L+3)m_0, n_0)$ and $(m_0, (2k+1)n_0)$ can be obtained respectively by use of the mode (m_0, n_0) and $((2L+1)m_0, n_0)$; $(2m_0, 2n_0)$ and $(2m_0, 2kn_0)$; $(2m_0, 2n_0)$ and $((2L+1)m_0, n_0)$; $(0, 2n_0)$ and $(m_0, (2k-1)n_0)$, respectively with the help of the linear terms $\sum\limits_{\substack{p+q=m\\ i+j=n}} (Pj-qi)\varphi_{pi}\theta_{qj}$, $\sum\limits_{\substack{|p-q|=m\\ i+j=n}} (Pj+qi)\varphi_{pi}\theta_{qj}$, $\sum\limits_{\substack{p+q=m\\ |i-j|=n}} (Pj+qi)\varphi_{pi}\theta_{qj}$, $\sum\limits_{\substack{|p-q|=m\\ i+j=n}} (Pj+qi)\varphi_{pi}\theta_{qj}$. Thus, $\Lambda'_{K+1,L+1}$ can be derived from $\Lambda'_{K,L}$, and let $K\to\infty$ and $L\to\infty$ and we obtain Eq. (A1) according to the inductive assumption given above.

REFERENCES

[1] Davis, S. H. (1967), Convection in a box: linear theory, *J. Fluid Mech.*, **30**: 465—478.

[2] Stork, K. and Müller, U. (1972), Convection in boxes: experiments, *ibid.*, **54**: 599—611.

[3] Platten, J. K. and Legros, J. C. (1984), *Convection in Liquids*, Springer, Berlin, 678 pp.

[4] Ahlers, G. and Behringer, R. P. (1978), The Rayleigh-Benard instability and the evolution of turbulence, *Suppl. Prog. Theor. Phys.*, No. 64: 186—201.

[5] Gollub, J. P. and Benson, S. V. (1980), Many routes to turbulent convection, *J. Fluid Mech.*, **100**: 449—470.

[6] Feigenbaum, M. J. (1978), Quantitative universality for a class of nonlinear transformations, *J. Stat. Phys.*, **19**: 25—52. ——(1979), The Universal metric properties of nonlinear transformations, *ibid.* **21**: 669—705.

[7] Ruelle, D. and Takens, F. (1971), On the nature of turbulence, *Commun. Math. Phys.*, **20**: 167—192.

[8] Newhouse, S., Ruelle, D. and Takens, F. (1978), Occurrence of strange Axiom A attractors near quasi-periodic flows on T^m, $m \geqslant 3$, *ibid.*, **64**: 35—40.

[9] Pomeau, Y. and Manneville, P. (1980), Intermittent transition to turbulence in dissipative systems, *ibid.*, **74**: 189—197.

[10] Curry, J. H. (1978), A generalized Lorenz System, *ibid.*, **60**: 193—204.

[11] Zhong Wenyi and Yang Peicai (1986), The transition of a multi-dimensional Loreng system, *Adv. Atmos. Sci.*, **3**: 289—301.

[12] Saltzman, B. (1962), Finite amplitude free convection as an initial value problem—I, *J. Atmos. Sci.*, **19**: 329—341.

[13] Curry, J. H., Herring, J. R., Loncaric, J. and Orszag, S. V. (1984), Order and disorder in two- and three-dimensional Benard convection, *J. Fluid Mech.*, **147**: 1—38.

[14] Sparrow. C. (1982), *The Lorenz Equation: Bifurcation, Chaos and Strange Attractors*, Springer-Verlag, New York, 267 pp.

[15] Lorenz, E. N. (1963), Determinitic non-periodic flow, *J. Atmos. Sci.*, **30**: 130—141.

[16] Qin Yuanxun (1958), *General Problems about Motion Stability*, Science Press, Beijing, 449 pp (in Chinese).

[17] Kubicek, M. and Marek, M. (1983), *Computational Methods in Bifurcation Theory and Dissipative Structures*, Springer-Verlag, New York, 243 pp.

[18] Kou, H. L. (1961), Solution of the non-linear equations of cellular convection and heat transport, *J. Fluid Mech.*, **10**: 611—634.

[19] Franceschini, V. and Tebaldi, C. (1984), Breaking and disappearance of tori, *Commun. Math. Phys.*, **94**: 317—329.

[20] Franceschini, V. (1983), Bifurcation of tori and phase locking in a dissipative system of differential equations, *Physica*, **6D**: 285—304.

[21] Gibbon, J. D. (1981), Dispersive instabilities in nonlinear systems: the real and complex Lorenz equation, In: Chaos and Order in Nature, *Proc. Intern. Sympo Synerg.*, Schlob Elmou, Bavaria, 92—101.